Antiwindup Input–Output Linearization Strategy for the Control of a Multistage Continuous Fermenter With Input Constraints

Céline Casenave, Marc Perez, Denis Dochain, Jérôme Harmand, Alain Rapaport, and Jean-Marie Sablayrolles

***Abstract*— This paper deals with the control of a multistage continuous fermenter (MSCF) used for the study of wine fermentation. The control design is facing three main difficulties: 1) system nonlinearity; 2) lack of online measurement of the controlled variable (sugar concentration); and 3) positive constraints on the control inputs (inlet flow rates of each tank) coming from the cascade structure of the system. A control strategy has been proposed, which accounts for these specificities. It is based on an input–output linearization control law coupled with an antiwindup technique and a state observer (the Kalman filter). The strategy has been tested and validated first on numerical simulations and then applied to the real process. The experiments gave satisfactory results that open up new perspectives on the use of the MSCF.**

***Index Terms*— Antiwindup, cascade of reactors, control design, input–output linearization, varying input constraints, wine fermentation.**

I. Introduction

IN THIS paper, we consider the problem of the control of a multistage continuous fermenter (MSCF) used for the study of wine fermentation. The experimental setup is a set of four reactors connected in series (see Fig. 1). The objective is to control the sugar concentration in each reactor by considering the input flow rates of the reactors as control inputs. The cascade structure of the system implies a constraint on the values of each control input. Indeed, the inlet flow rate of each reactor has to be lower than that of the preceding reactor (i.e., $Q_{i+1} \leqslant Q_i$). This constraint as well as the process nonlinearity make the control design complex and not trivial.

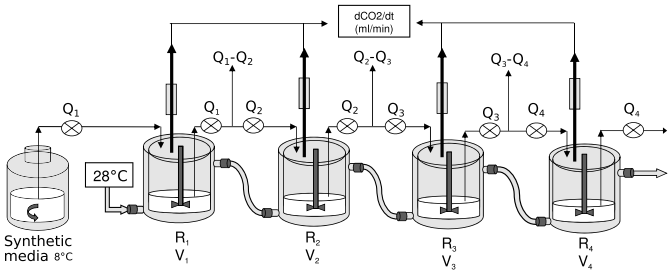

Fig. 1. Scheme of the MSCF.

The control of continuous bioreactors has been widely studied in the automatic control literature [1] with numerous applications on bioengineering processes (e.g., [2]). In comparison, only few papers deal with the issue of the control of a cascade of bioreactors (see [3], [4]), whereas such kind of devices is often used in the industrial engineering processes (e.g., [5]). Moreover, only a scalar variable is generally controlled in these papers. For example, Vigie *et al.* [3] design a controller for the glucose concentration in the process outlet. And in [4], the objective is to maximize the biogas flow rate of the first reactor in a two-stage anaerobic bioreactor, the second reactor being not controlled.

Constraints on the values of control inputs are often encountered in practice. One classical constraint is the saturation constraint with lower and upper limits on the control input u: $u_m \leqslant u(t) \leqslant u_M$. The control of systems subject to saturation is the topic of numerous studies, in the case of both linear and nonlinear systems. There are generally two ways to deal with such issue: either we first design a controller without taking the constraints into account, and then, we try to compensate the effect of the saturation (this is the case of the antiwindup techniques [6]), or we include the saturation from the beginning of the design process, as it is the case with set invariance control design [7] or techniques based on the polytopic representation of the saturation [8], [9]. However, these techniques are only suitable for constraints of saturation type with constant bounds. For more general forms of constraints, it is sometimes possible to make a change of variable for the control input so that the constraint on the new input variable

Manuscript received August 31, 2018; accepted December 25, 2018. Manuscript received in final form January 10, 2019. This work was supported in part by the 7th Framework Program of the European Union through the Computer-Aided Food Processes for Control Engineering Project–Large Collaborative Project under Grant KBBE-2007-2-3-01 and in part by the Caractérisation et élaboration des produits issus de l'agriculture (CEPIA) Division of French National Institute for Agricultural Research (INRA). Recommended by Associate Editor W. He. *(Corresponding author: Céline Casenave.)*

C. Casenave and A. Rapaport are with the Research Unit Mathematics, Informatics and STatistics for Environment and Agronomy (MISTEA), Université de Montpellier, French National Institute for Agricultural Research (INRA), Montpellier SupAgro, 34060 Montpellier, France (e-mail: celine.casenave@inra.fr; alain.rapaport@inra.fr).

M. Perez and J.-M. Sablayrolles are with the Research Unit Sciences for Oenology (SPO), Université de Montpellier, French National Institute for Agricultural Research (INRA), Montpellier SupAgro, 34060 Montpellier, France (e-mail: marc.perez@inra.fr; jean-marie.sablayrolles@inra.fr).

D. Dochain is with the Institute of Information and Communication Technologies, Electronics and Applied Mathematics (ICTEAM), Université Catholique de Louvain (UCL), 1348 Ottignies-Louvain-la-Neuve, Belgium (e-mail: denis.dochain@uclouvain.be).

J. Harmand is with the Laboratory of Environmental Biotechnology (LBE), Université de Montpellier, French National Institute for Agricultural Research (INRA), 11100 Narbonne, France (e-mail: jerome.harmand@inra.fr).

Digital Object Identifier 10.1109/TCST.2019.2892932

is a saturation. For example, the constraint $0 \leqslant Q_2 \leqslant Q_1 \leqslant Q_{\max}$ can be replaced by $0 \leqslant Q_1 \leqslant Q_{\max}$ and $0 \leqslant \alpha \leqslant 1$, where α is such that $Q_2 = \alpha Q_1$. However, when doing so, the structure of the system is modified and often no more adapted to classical control techniques that are dedicated to particular form of systems, such as control-affine systems.

Finally, it is not obvious to find control design techniques that are adapted to nonlinear systems with general positive input constraints. Doyle [10] proposes to combine two techniques: the feedback linearizing control for nonlinear systems [11] and an antiwindup technique [12] for linear systems which has the advantage to handle the case of saturations with time-varying bounds. In the present paper, this control strategy has been coupled with a state observer and then, applied to the MSCF. The closed-loop system behaves appropriately and stabilizes faster than or at least at the same speed as when a constant input is applied. The control strategy has been validated both in numerical simulation and on the experimental process. The first version of this strategy and the results obtained during the first set of experiments were presented at the IFAC World Congress [13].[1]

This paper is organized as follows. In Section II, the experimental setup is described. The model used for the design of the control law is presented and analyzed in Section III. In Section IV, the model parameters are identified and the numerical simulations are compared with experimental data for validation. Then, Section V deals with the design of the control strategy. Finally, in Section VI, the control results obtained in simulation and on the experimental process are presented.

II. Process Description

In [14], the use of an MSCF has been proposed to study the fermentation process. An experimental setup has been developed by the research unit Sciences for Oenology (SPO), French National Institute for Agricultural Research, Montpellier, France. It is composed of four reactors connected in series (see Fig. 1). The volumes V_i, $i = 1:4$, of the reactors are kept constant. This implies that the outlet flow rate of each reactor is equal to its inlet flow rate. The first reactor is fed with a synthetic medium, which simulates a grape juice. The other reactors are fed by a fraction of the outlet medium of the preceding reactor. The inlet flow rates $Q_i, i = 1:4$, of the reactors are controlled independently by a pump, the only constraint (coming from the cascade structure of the device) being that the inlet flow rate Q_i of the ith reactor has to be lower than the outlet flow rate Q_{i-1} of the $(i-1)$th reactor

$$0 \leqslant Q_4 \leqslant Q_3 \leqslant Q_2 \leqslant Q_1 \leqslant Q_{\max} \tag{1}$$

with $Q_{\max}$ the maximal flow rate that can be applied.

The temperature of the medium in each reactor is controlled at 28 °C. Only the CO_2 production rate (in each of the four reactors) is measured online. A schematic view of the MSCF is given in Fig. 1.

[1]The paper did receive the congress Application Paper Prize.

III. Model Description and Analysis

The model of the MSCF considered in this paper is the one described in [13]. It is obtained from the model of the batch fermentation given in [15] by addition of the terms related to the interconnection between the reactors. It is written

$$\dot{\xi} = f(\xi, u) \text{ with } \xi = \left(\xi_1^\mathsf{T}, \xi_2^\mathsf{T}, \xi_3^\mathsf{T}, \xi_4^\mathsf{T}\right)^\mathsf{T} \tag{2}$$

and $\xi_i = (X_i, N_i, E_i, S_i)^\mathsf{T}$, $u = (D_1, D_2, D_3, D_4)^\mathsf{T}$, $f(\xi, u) = (f_1(\xi, u)^\mathsf{T}, f_2(\xi, u)^\mathsf{T}, f_3(\xi, u)^\mathsf{T}, f_4(\xi, u)^\mathsf{T})^\mathsf{T}$, and $\forall i = 1:4$

$$f_i(\xi, u) := \begin{bmatrix} \mu_1(N_i)X_i + D_i(X_{i-1} - X_i) \\ -k_1\mu_1(N_i)X_i + D_i(N_{i-1} - N_i) \\ \mu_2(E_i, S_i)X_i + D_i(E_{i-1} - E_i) \\ -k_2\mu_2(E_i, S_i)X_i + D_i(S_{i-1} - S_i) \end{bmatrix} \tag{3}$$

where X_i, N_i, E_i, and S_i are the concentrations (in g.L^{-1}) of yeast, nitrogen, ethanol, and sugar of the ith reactor, respectively; $D_i = (Q_i/V_i)$ is the dilution rate of the ith reactor; $(X_0, N_0, E_0, S_0) = (0, N^{\text{in}}, 0, S^{\text{in}})$ with N^{in}, $S^{\text{in}} > 0$ are the concentrations of yeast, nitrogen, ethanol, and sugar in the inlet medium; and k_1 and k_2 are the yield coefficients. The functions μ_1 and μ_2 are given by

$$\mu_1(N) = \frac{\mu_1^{\max} N}{K_N + N}, \quad \mu_2(E, S) = \frac{\mu_2^{\max} S}{K_S + S}\frac{K_E}{K_E + E} \tag{4}$$

with $\mu_1^{\max}$, $\mu_2^{\max}$, K_S, K_N, and K_E the maximum specific growth rates of the two reactions, the half-saturation constants of the Monod laws, and the inhibition constant, respectively. To complete the model, the following initial conditions are considered, $\forall i = 1:4$:

$$X_i(0) = X^{\text{in}}, \quad N_i(0) = N^{\text{in}}, \quad E_i(0) = 0, \quad S_i(0) = S^{\text{in}}. \tag{5}$$

We also denote C_i the CO_2 production rate of the ith reactor

$$C_i(\xi) := \mu_2(E_i, S_i)X_i. \tag{6}$$

Let us now give a few analysis results about the MSCF model (2). The goal is only to show that the model is consistent with some biological laws and experimental observations. The proofs of the results, long but only technical, are not given in this paper.

By simple computations, we can first show that the set Ω defined by

$$\Omega := \left\{ \xi \in \mathbb{R}^{16} \text{ such that } \begin{cases} 0 \leqslant X_i \leqslant \frac{N^{\text{in}} - N_i}{k_1} \\ 0 \leqslant N_i \leqslant N^{\text{in}} \\ 0 \leqslant E_i \leqslant \frac{S^{\text{in}} - S_i}{k_2} \\ 0 \leqslant S_i \leqslant S^{\text{in}} \end{cases} \right\} \subset \mathbb{R}^{16}_+ \tag{7}$$

(with $\mathbb{R}^{16}_+ = [0, +\infty[^{16}$), is a positive invariant set of system (2), which proves its consistency with the mass balance conservation law.

One can also easily show that, if $(Q_1/V_1) < \mu_1(N^{\text{in}})$, then the system (2) admits a unique positive and locally exponentially stable steady state $\xi^* \in \Omega$; moreover, this steady state is such that

$$0 < S_i^* < S_{i-1}^* \text{ and } X_i^* > X_{i-1}^*, \quad \forall i = 1:4 \tag{8}$$

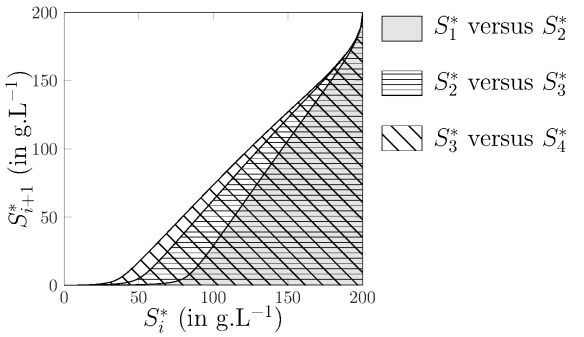

Fig. 2. Example of set of reachable values of sugar concentrations at equilibrium in the MSCF.

TABLE I

ESTIMATED VALUES OF THE YIELD COEFFICIENT $k_2 = (E/S^{\text{IN}} - S)$ FROM MEASURED VALUES OF E AND S DURING A BATCH FERMENTATION. $k_2^{(1)}$ IS OBTAINED WITH $S^{\text{IN}} = 200$ G.L^{-1} AND $k_2^{(2)}$ WITH $S^{\text{IN}} = 195.8$ G.L^{-1}

t [h]	16.4	20.9	24.0	26.1	40.5	45.7	49.4	65.4	74.9
$k_2^{(1)}$	0.339	0.432	0.434	0.437	0.464	0.457	0.461	0.463	0.463
$k_2^{(2)}$	0.449	0.494	0.472	0.468	0.480	0.470	0.473	0.474	0.473

with $S_0^* = S^{\text{in}}$ and $X_0^* = X^{\text{in}}$. It means that, providing that $Q_{\max} < V_1\mu_1(N^{\text{in}})$, all inlet flow rate values (Q_1, Q_2, Q_3, Q_4) that meet the constraint (1) will make the system stabilize at a positive equilibrium point without any washout in all the reactors ($X_i^* \neq 0$, $\forall i$).

However, given $(\bar{S}_1, \bar{S}_2, \bar{S}_3, \bar{S}_4) \in [0, S^{\text{in}}]^4$ with $\bar{S}_1 > \bar{S}_2 > \bar{S}_3 > \bar{S}_4$, it does not necessarily exist some values $(Q_1, Q_2, Q_3, Q_4) \in [0, V_1\mu_1(N^{\text{in}})]^4$ with $Q_4 \leqslant Q_3 \leqslant Q_2 \leqslant Q_1$, such that the equilibrium point ξ^* of system (2) verifies $S_i^* = \bar{S}_i, \forall i = 1:4$. An example of set of reachable values of sugar concentrations is given in Fig. 2.

IV. MODEL IDENTIFICATION

Let us first focus on the estimation of the value of the initial sugar concentration S^{in} that plays a key role. In the model of the batch fermentation [model (2) with $D_i = 0$], it is assumed that the yield coefficient k_2 is constant during the fermentation. However, it is well known in the field of Oenology that k_2 varies; in particular, it is smaller at the beginning of the fermentation (see Table I). Fortunately, this variation of k_2 can be artificially attenuated by a modification of the value of S^{in} in the model. Indeed, at the beginning of the fermentation, the quantity $S^{\text{in}} - S$, which represents the concentration of sugar that has been consumed, is small. A slight decrease of the value of S_{in} will then lead to an increase of the value of $k_2 = (E/S^{\text{in}} - S)$ larger than the increase obtained at the end of the fermentation, where the value of $S^{\text{in}} - S$ is large (close to S^{in}). By slightly decreasing the value of S^{in} in the model, we can therefore keep a constant value of k_2 without degrading too much the accuracy of the model.

In the case of the batch fermentation data set considered in Table I, the value of S^{in} that enables to attenuate at best the variation of k_2 is equal to 195.8 g.L^{-1}, which is 4.2 g.L^{-1} smaller than the real value of 200 g.L^{-1}. This value, denoted

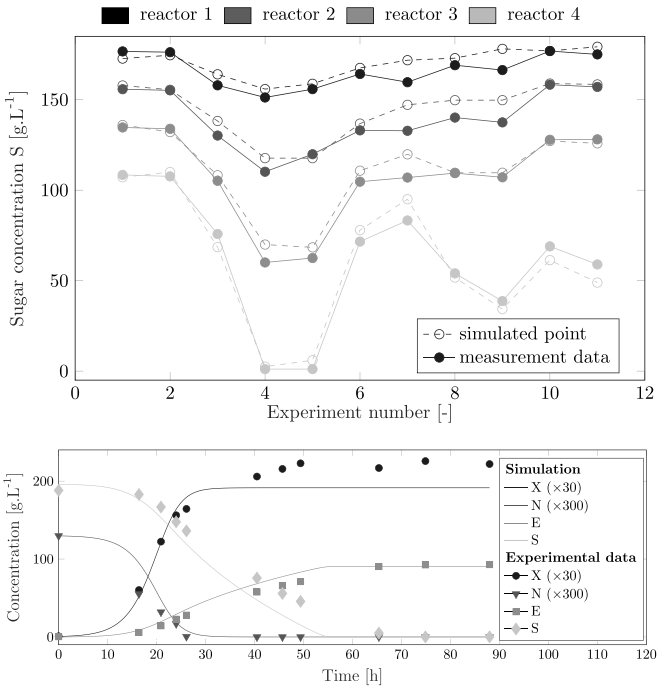

Fig. 3. Comparison between experimental data and simulations of the models of fermentation (batch and MSCF). Top: sugar concentration values at equilibrium in the MSCF. The experimental data are the ones used for the identification process. Bottom: yeast, nitrogen, ethanol, and sugar concentrations of a batch fermentation (cross validation).

$\bar{S}^{\text{in}}$ in the sequel, has been obtained by simple linear regression between S and E ($R^2 = 0.999$) based on the relationship $S = S^{\text{in}} - k_2 E$.

For the parameter identification, we used a data set collected by the unit SPO [14]. Each experiment consisted in the application of a set of constant inlet flow rates Q_i, $i = 1:4$ that fulfill the constraint (1); after stabilization, the equilibrium values of the concentrations of yeast, sugar, ethanol, and nitrogen were measured.

The value of parameter k_2 was considered as known, as it is a stoichiometric coefficient of a well-known chemical reaction; we used the value given in [15]. The other parameters of model (2) were identified from the experimental data; a simplex method was used to minimize the sum of the squares of the distances between the experimental measurements at equilibrium in the four stages of the MSCF and the values obtained by numerical simulation of the model. Because the equations of the nitrogen and yeast concentrations are independent of the other ones, the identification was performed in two steps.

1) First, the coefficients k_n, k_1, and $\mu_1^{\max}$ were identified from the measurements of the yeast concentrations.
2) Then, the coefficients k_s, k_e, and $\mu_2^{\max}$ were identified from the measurements of the sugar concentrations.

The values of the identified parameters are given hereafter[2]

$$\begin{aligned} k_1 = 0.068, \quad k_2 = 2.17, \quad \mu_1^{\max} = 0.75\ [\text{h}^{-1}] \\ \mu_2^{\max} = 1.746\ [\text{h}^{-1}],\ k_n = 0.714\ [\text{g.L}^{-1}] \\ k_s = 0.884\ [\text{g.L}^{-1}],\ k_e = 13.8\ [\text{g.L}^{-1}]. \end{aligned} \tag{9}$$

[2] k_1 and k_2 are dimensionless parameters.

The comparison between the experimental data used for the identification process and the values obtained by simulation with the parameter values (9) is given in Fig. 3 (top). For the cross validation, we compared simulated trajectories of a batch fermentation with experimental data [see Fig. 3 (bottom)]. In both cases, the simulation gives results close to the measured values.

V. Design of the Control Law

Recall that the objective is to control the sugar concentration in each stage of the MSCF, the control inputs being the inlet flow rates $Q_i,\ i = 1:4$, of the four reactors. In the sequel, let denote S_i^* the value of the sugar concentration set-point in the ith reactor (for $i = 1:4$). We only consider set-point values, such that there exist constant input control values $(Q_1^*, Q_2^*, Q_3^*, Q_4^*) \in [0, Q_{\max}]^4$, verifying the constraint (1) and which, when applied to the system (2), stabilize the sugar concentrations in the four reactors at the values $S_i^*,\ i = 1:4$. This implies that $S^{\text{in}} > S_1^* > S_2^* > S_3^* > S_4^* > 0$ and $Q_{\max} < V_1\mu_1(N^{\text{in}})$ (see Section III). Thus, after stabilization, it is possible to switch to constant input flow rates in order to maintain the system in the same state without applying the closed-loop control law.

The control design is facing two main difficulties: on one hand, no online measurement of the sugar concentration is available, and on the other hand, the control inputs Q_i have to verify the constraint (1). The proposed control strategy is based on a linearizing control law, coupled with an antiwindup component and a state observer. A scheme of the control strategy is given in Fig. 4(b).

A. Linearizing Control Law

To account for the system nonlinearities, a linearizing control law is considered. The equation of S_i has a relative degree equal to 1 with respect to Q_i; the control law is therefore written[3]

$$Q_i = V_i\frac{k_2C_i + \upsilon_i}{S_{i-1} - S_i} := \Psi_i(\upsilon_i, S, C) \tag{10}$$

where $C = (C_1, C_2, C_3, C_4)^\intercal$, $S = (S_1, S_2, S_3, S_4)^\intercal$, and υ_i is the expression of the desired closed-loop dynamics of S_i. Here, we consider a simple proportional-integral linear dynamics

$$\upsilon_i = a_{i,1}\big(S_i^* - S_i\big) + a_{i,2}\int_0^t \big(S_i^* - S_i(\tau)\big)d\tau \tag{11}$$

with $a_{i,1}$ and $a_{i,2}$ some positive constants. The integral term is introduced to compensate the modeling and measurement errors. Note that the control law (10) is independent of the function μ_2 because the quantity C_i is measured online.

B. Saturation

Consider the saturation operator defined by

$$\text{sat}(u; u_m, u_M) := \begin{cases} u_M & \text{if } u \geqslant u_M \\ u & \text{if } u_m < u < u_M \\ u_m & \text{if } u \leqslant u_m. \end{cases} \tag{12}$$

[3]Note that this control law cannot be applied if $S_i = S_{i-1}$, case that never happens except at the very beginning of the experiments when the reactors are filled with the must and then connected to each other.

TABLE II
14 Possible Saturation Orders

	1	2	3	4	5	6	7	8	9	10	11	12	13	14
n_1	1	1	1	1	1	2	2	2	3	2	2	3	4	3
n_2	2	2	3	3	4	1	1	3	2	3	4	2	3	4
n_3	3	4	2	4	3	2	3	1	1	4	3	3	2	2
n_4	4	3	3	2	2	3	2	2	2	1	1	1	1	1

Compared to the problems often considered in the literature, the constraints on the control inputs of our system are coupled and time varying. We chose to apply the saturation operator (12) to one control input after the other. The choice of the saturation order of the four control inputs Q_i is not obvious; it can lead to very different control performances, depending on the set-points, the initial conditions, and the experimental conditions. The 14 possible saturation orders are given in Table II; $n_i = j$ meaning that Q_i will be the jth control input to be saturated.

For example, the order $n°8$ has to be understood as follows:

1. $n_3 = 1 \Longrightarrow \tilde{Q}_3 = \text{sat}(Q_3; 0, Q_{\max})$
2. $n_1 = n_4 = 2 \Longrightarrow \begin{cases} \tilde{Q}_1 = & \text{sat}(Q_1; \tilde{Q}_3, Q_{\max}) \\ \tilde{Q}_4 = & \text{sat}(Q_4; 0, \tilde{Q}_3) \end{cases}$
3. $n_2 = 3 \Longrightarrow \tilde{Q}_2 = \text{sat}(Q_2; \tilde{Q}_3, \tilde{Q}_1)$.

This saturation strategy can be written as follows:

$$\tilde{Q}_i = \text{sat}(Q_i; Q_{i,m}, Q_{i,M}) \tag{13}$$

where $Q_{i,m} = \max_{j>i, n_j<n_i} \tilde{Q}_j$ and $Q_{i,M} = \min_{j<i, n_j<n_i} \tilde{Q}_j$ with $\tilde{Q}_5 = 0$, $\tilde{Q}_0 = Q_{\max}$, and $n_0 = n_5 = 0$.

C. Antiwindup

Enforcing input control constraints by the application of a saturation operator can result in poor closed-loop performances and overshooting of the integral term. To minimize the performance loss, some antiwindup control schemes have been developed. However, the problems studied in the literature are, most of the time, linear. An interesting solution for nonlinear systems was proposed in [10]. It is based on the combination of two techniques: the feedback linearizing control for nonlinear systems [11], and the antiwindup technique developed by Zheng *et al.* [12], which has the advantage to handle the case of saturations with time-variable bounds. The combined scheme is explained hereafter.

1) Antiwindup Technique of Zheng et al. [12] for Linear Systems: Consider a linear and stable square system of transfer function P that is subject to input saturation constraint[4]

$$y = P\tilde{u} \text{ with } \tilde{u} = \text{sat}(u; u_m, u_M) \tag{14}$$

where y, u, and $\tilde{u}$ are the output, input, and saturated input of the system, respectively. Let K be a feedback controller designed on the unconstrained system [see Fig. 4(a)], r the set-point, and F a diagonal filter, such that FP is biproper

[4]In the sequel, by an abuse of notation and for simplicity, the Laplace transform of a function f will be denoted itself by f when there is no ambiguity.

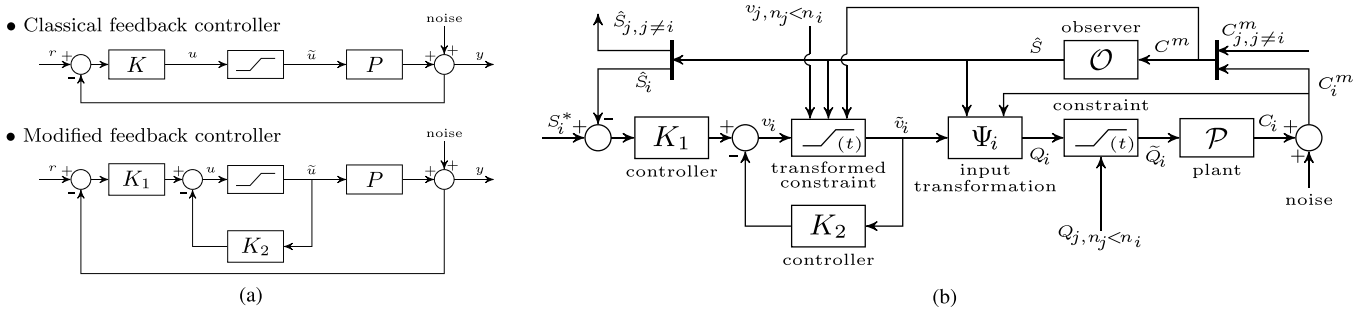

Fig. 4. Schemes of control strategies. (a) Antiwindup scheme [12] for linear systems. (b) Complete control strategy scheme of the ith reactor.

(that is, a rational function with the same numerator and denominator degrees). The input $\tilde{u}$ that fulfills the saturation constraint and which is such that at each time t

$$\tilde{u}(t) = \arg\min_{\tilde{v}(t)} |[FP(I+KP)^{-1}Kr](t) - [FP\tilde{v}](t)|_1 \quad (15)$$

is given by [see Fig. 4(a)]

$$\tilde{u} = \text{sat}(K_1(r-y) - K_2\tilde{u}; u_m, u_M) \quad (16)$$

with $K_1 = FP(I+KP)^{-1}K$ and $K_2 = FP - I - K_1P$. At each time instant, this saturated control input minimizes the difference between the output of the closed-loop system without saturation and the output of the system obtained with the saturated input.

To guarantee the internal stability of the closed-loop system and the implementability of the controller, the following assumptions have to be verified.

- $(I+KP)^{-1}K$ is biproper, minimum phase, and stable.
- $FP_{|s=\infty}$ is a diagonal nonsingular matrix with finite elements.
- K_1 is minimum phase and stable.
- $K_1P + K_2$ is strictly proper.

2) Adaptation to Nonlinear Systems by Doyle [10]: Let us now consider affine nonlinear SISO systems of the form

$$\frac{dx}{dt} = f(x) + g(x)u;\ y = h(x) \quad (17)$$

subject to input saturation: $u_m \leqslant u \leqslant u_M$.

The first step of the control strategy is an input–output linearization that consists in a change of input variable of the form

$$u = f_1(x) + f_2(x)v \quad (18)$$

where f_1 and f_2 are chosen in such a way that the system with input v and output y is linear: $y = Pv$ with P as a rational transfer function.

Then, the initial constraint on u is transformed in a constraint on v in the following way:

$$\begin{aligned} &u_m \leqslant u := f_1(x) + f_2(x)v \leqslant u_M \\ \Leftrightarrow\ &\frac{u_m - f_1(x)}{f_2(x)} \leqslant v \leqslant \frac{u_M - f_1(x)}{f_2(x)}. \end{aligned} \quad (19)$$

Finally, the antiwindup scheme proposed by Zheng *et al.* [12] is applied to the linear system $y = Pv$ with the time-varying input constraint (19).

3) Application to the MSCF: The input–output linearization, already presented in Section V-A, is obtained with the change of variables (10) which is of the form (18) with $f_1(x) = V_i(k_2C_i/S_{i-1} - S_i)$ and $f_2(x) = (V_i/S_{i-1} - S_i)$. The resulting transfer function between v_i and S_i is $P(s) = (1/s)$.

The constraint on Q_i is then transformed into a constraint on v_i

$$\begin{aligned} &Q_{i,m} < Q_i < Q_{i,M} \\ \Leftrightarrow\ &\underbrace{\frac{S_{i-1} - S_i}{V_i}Q_{i,m} - k_2C_i}_{v_{i,m}} < v_i < \underbrace{\frac{S_{i-1} - S_i}{V_i}Q_{i,M} - k_2C_i}_{v_{i,M}}. \end{aligned} \quad (20)$$

To apply the antiwindup scheme of Zheng *et al.* [12] to the linear system of transfer function $P(s) = (1/s)$ with the input saturation constraint (20), we first have to consider a feedback controller for the unconstrained problem. The controller we have chosen is the one expressed in (11), which is written in the frequency domain

$$v_i = K\left(S_i^* - S_i\right) \text{ with } K(s) = \frac{a_{i,1}s + a_{i,2}}{s}. \quad (21)$$

Several controllers for the constrained problem can then be proposed, following the method of Zheng *et al.* [12]. The choice of $F(s) = a_{i,1}(s^2 + a_{i,1}s + a_{i,2}/a_{i,1}s + a_{i,2})$ leads to the following controllers:

$$K_1 = FP(I+KP)^{-1}K = a_{i,1} \quad (22)$$

$$K_2 = FP - I - K_1P = -\frac{a_{i,2}}{a_{i,1}s + a_{i,2}} \quad (23)$$

which check all the assumptions required provided that $a_{i,1}, a_{i,2} > 0$.

By applying the same saturation order as for the Q_i values ($i = 1:4$), we then finally have

$$\tilde{v}_i = \text{sat}(v_i; v_{i,m}, v_{i,M}) \text{ with } v_i = K_1\left(S_i^* - S_i\right) - K_2\tilde{v}_i. \quad (24)$$

D. Observer

The antiwindup control scheme presented earlier assumes a full knowledge of both the sugar concentrations S_i and the CO_2 production rate C_i in each reactor. However, only the CO_2 production rate is measured online. To get an online estimate of the sugar concentration, we need to use a state observer. Several observation strategies (among which,

the asymptotic observer [13] and the extended Kalman filter) have been tested numerically, which all give similar results. They also all have the same drawback; the convergence rate is always limited by the value of D_i.

Finally, we chose to use a continuous-discrete extended Kalman filter (see [16, p.664]), as it seemed to handle better uncertainties on the observer initial condition. This approach is dedicated to continuous-time model of the form (2) with an additional discrete-time measurement output equation of the form

$$C_k^m = C(\xi(t_k)) + \eta_k \tag{25}$$

where, in our case, $C(\xi) = (C_1(\xi), C_2(\xi), C_3(\xi), C_4(\xi))^\intercal$, and η_k is a Gaussian measurement noise of zero mean and covariance matrix R_k assumed to be equal to $R_k = \sigma I_4$ with $\sigma > 0$ (I_4 being the identity matrix of size 4×4). No noise was added in the model equations. At each time instant t_k, the Kalman filter computes an estimation of the state $\hat{\xi}_k^+$ and the error covariance matrix P_k^+ in two steps: a first step of prediction based on the model and the previous estimated values and a second step of correction based on the measurement.

For the initial value of the state estimate $\hat{\xi}_0^+$, we took advantage of the fact that at the observer initialization time $t_k = 0$, the system is assumed to be at equilibrium. Indeed, in practice, the control law will be used to go from one equilibrium point to another. Under this assumption, we get from (2) the following estimation $\hat{\xi}_0^+$ of $\xi(0)$:

$$\hat{\xi}_0^+ = \left(\hat{\xi}_{1,0}^\intercal, \hat{\xi}_{2,0}^\intercal, \hat{\xi}_{3,0}^\intercal, \hat{\xi}_{4,0}^\intercal\right)^\intercal \text{ with } \hat{\xi}_{i,0} = \left(\hat{X}_i^0, \hat{N}_i^0, \hat{E}_i^0, \hat{S}_i^0\right)^\intercal \tag{26}$$

and $\forall i = 1:4$

$$\hat{S}_i^0 = -k_2 \frac{C_i^m(0)}{D_i(0)} + \hat{S}_{i-1}^0, \quad \hat{E}_i^0 = \frac{C_i^m(0)}{D_i(0)} + \hat{E}_{i-1}^0 \tag{27}$$

$$\hat{X}_i^0 = \frac{C_i^m(0)}{\mu_2(\hat{E}_i^0, \hat{S}_i^0)}, \quad \hat{N}_i^0 = \frac{K_N D_i(0)\left(\hat{X}_i^0 - \hat{X}_{i-1}^0\right)}{\mu_1^{\max} \hat{X}_i^0 - D_i(0)\left(\hat{X}_i^0 - \hat{X}_{i-1}^0\right)} \tag{28}$$

where $C_i^m(0)$ is the measurement of $C_i(0)$, $\hat{S}_0^0 = S^{\text{in}}$, $\hat{E}_0^0 = 0$, and $\hat{X}_0^0 = 0$. The initial value P_0^+ has then been classically chosen equal to $\varepsilon \times P_0^2$ with $\varepsilon > 0$ and P_0 the 16×16 diagonal matrix whose diagonal vector is ξ_0^+.

In practice, some off-line measurements of the sugar concentration are available during the experiment. The information given by these measurements, even if they are available only a few hours after the sampling, can be used to adjust the estimation of the observer. It can be very useful, especially to correct the error made on the initial conditions of the observer. In the experiments presented in Section VI, three off-line measurements of the sugar concentrations are performed at different times. For another example, the reader can refer to the conference paper [13], where the adjustment of the observer (which is not a Kalman filter) is more visible.

E. Complete Control Strategy Scheme

Finally, the complete control strategy is written [Fig. 4(b)]

$$\hat{S}_i \quad \text{given by the Extended Kalman Filter} \tag{29}$$

$$\upsilon_i = K_1\left(S_i^* - \hat{S}_i\right) - K_2 \tilde{\upsilon}_i \tag{30}$$

$$\tilde{\upsilon}_i = \text{sat}(\upsilon_i; \upsilon_{i,m}, \upsilon_{i,M}) \tag{31}$$

$$Q_i = \Psi_i\left(\tilde{\upsilon}_i, \hat{S}, C^m\right) \tag{32}$$

$$\tilde{Q}_i = \text{sat}(Q_i; Q_{i,m}, Q_{i,M}). \tag{33}$$

It takes less than 4 ms to compute the value of the control input from the new online measurements of the CO_2 production rate.

VI. Numerical and Experimental Validations

The control strategy was validated in numerical simulations and applied to the experimental setup. The results are given hereafter.

A. Design of the Experiments

The considered MSCF has four reactors of respective volumes

$$(V_1, V_2, V_3, V_4) = (1, 0.8, 0.55, 0.7) \text{ [L]}. \tag{34}$$

The maximal value of inlet flow rate that can be applied is $Q_{\max} = 0.24$ L.h^{-1}. The synthetic media contain $S_{\text{in}} = 202$ g.L^{-1} of glucose (quantity measured at the beginning of the experiments) and $N_{\text{in}} = 0.425$ g.L^{-1} of assimilable nitrogen. At the beginning of the experiment, the yeasts are inoculated in each reactor with an initial concentration X_{in} of 10^6 cell/mL, which corresponds to 0.04 g.L^{-1} for the yeast strain used (commercial strain EC1118, Lallemand SA).

The set-point we consider for the experiments is the following one:

$$\left(S_1^*, S_2^*, S_3^*, S_4^*\right) = (170, 140, 110, 70) \text{ [g.L}^{-1}\text{]}. \tag{35}$$

Its reachability has been verified in simulation.

To avoid the case where $Q_{i+1} = Q_i$, for which we have observed a significant difference between the inlet flow rate values to be applied and the real measured inlet flow rates, the constraint (1) was replaced by the stronger following one:

$$Q_1 < Q_{\max} \text{ and } \forall i = 2:4, \quad 0 < Q_i < 0.9\, Q_{i-1}. \tag{36}$$

The saturation strategy (see Section V-B) was modified consequently.

We assume that when the control law is applied, the MSCF is at equilibrium, the constant dilution rates being equal to

$$\left(D_1^0, D_2^0, D_3^0, D_4^0\right) = (0.24, 0.26, 0.32, 0.05) \text{ [h}^{-1}\text{]}. \tag{37}$$

It corresponds to the following values of inlet flow rates:

$$\left(Q_1^0, Q_2^0, Q_3^0, Q_4^0\right) = (0.24, 0.208, 0.176, 0.035) \text{ [L.h}^{-1}\text{]} \tag{38}$$

that fulfill the constraint (36).

B. Online Measurements of the CO_2 Production Rate

The control strategy relies on the availability of an online measurement of the CO_2 production rate C in each stage of the MSCF. In our experiments, we measured the CO_2 present in the gas released in the air by the fermentation process, and we deduced from this measurement an estimation of the

CO_2 gaseous outflow rate (quantity of CO_2 released by unit of time); a new measurement is available every 20 min. We then assumed that at each time t, the CO_2 gaseous outflow rate is equal to the CO_2 production rate. However, it is well known that a part of the CO_2 produced by the degradation of sugar during the fermentation process is dissolved in the grape juice; this quantity can therefore not be measured from the produced gas that only contains the released CO_2. This bias on the measurement of the CO_2 induces an error on the estimation of the CO_2 production rate at the beginning of the fermentation when the medium is not saturated in CO_2. After this period, the CO_2 gaseous outflow rate gives a good estimation of the CO_2 production rate. We will see, in the sequel, how to compensate this error in the model.

The model of the batch fermentation [model (2) with $D_i = 0$] and the associated control strategy rely on a strong relationship between the sugar concentration S and the CO_2; we indeed have

$$\forall t > 0, \quad \frac{dS}{dt} = -k_2 \frac{d\mathrm{CO}_2}{dt} \Leftrightarrow S(t) = \bar{S}^{\mathrm{in}} - k_2 \mathrm{CO}_2(t). \quad (39)$$

Thus, a measurement error made on $CO_2(t)$ directly impacts the estimation of $S(t)$. Let us denote by c_d the quantity of CO_2 dissolved in the medium (in $\mathrm{g.L}^{-1}$) and ${\mathrm{CO}_2}^m(t)$ the measured value of CO_2 at time t; then, we have $\mathrm{CO}_2(t) = {\mathrm{CO}_2}^m(t) + c_d$, which leads to

$$S(t) = \tilde{S}^{\mathrm{in}} - k_2 {\mathrm{CO}_2}^m(t) \text{ with } \tilde{S}^{\mathrm{in}} = \bar{S}^{\mathrm{in}} - k_2 c_d. \quad (40)$$

By removing from $\bar{S}^{\mathrm{in}}$ the quantity of sugar corresponding to the quantity of dissolved CO_2, we can therefore compensate the measurement error on CO_2 providing that we know the value of c_d.

To obtain an order of magnitude of c_d, we can perform a linear regression between E and ${\mathrm{CO}_2}^m$ based on the relationship $E = \mathrm{CO}_2 = {\mathrm{CO}_2}^m(t) + c_d$. Indeed, the measurement of the ethanol concentration is not biased on the contrary of the measurement of CO_2. The least squares regression performed on the batch fermentation data set of Fig. 3 leads to the value of $c_d = 3.99$ $\mathrm{g.L}^{-1}$ with $R^2 = 0.9985$, which corresponds to a sugar concentration value $k_2 c_d = 8.7$ $\mathrm{g.L}^{-1}$. To compensate the measurement bias on CO_2 in the model, we can therefore decrease the value of $\bar{S}^{\mathrm{in}}$ of 8.7 $\mathrm{g.L}^{-1}$. Recall that $\bar{S}^{\mathrm{in}}$ was obtained from S^{in} by subtraction of 4.2 $\mathrm{g.L}^{-1}$ to attenuate the variability of k_2 (see Section IV). Thus, the quantity $\tilde{S}^{\mathrm{in}}$ can be seen as a corrected value of S^{in} that takes into account two corrections: a first one to attenuate the variability of k_2 and a second one to compensate the measurement bias on CO_2.

As the MSCF behaves slightly differently from the batch fermentation process, a new value of $\bar{S}^{\mathrm{in}}$ has been computed from the data set obtained with the MSCF. In Fig. 5, the measured CO_2 gaseous outflow rate is plotted versus the fermentation progress $1 - S/S^{\mathrm{in}}$, where $S^{\mathrm{in}} = 202$ $\mathrm{g.L}^{-1}$. The value of S was either measured or estimated. The measurements of S were mainly made at equilibrium in the different reactors of the MSCF, except for one measurement performed at the end of the growth phase during a batch fermentation. The estimated values of S during a batch fermentation were deduced from ${\mathrm{CO}_2}^m$ by the formula $S = \tilde{S}^{\mathrm{in}} - k_2 {\mathrm{CO}_2}^m$ for two values of $\tilde{S}^{\mathrm{in}}$:

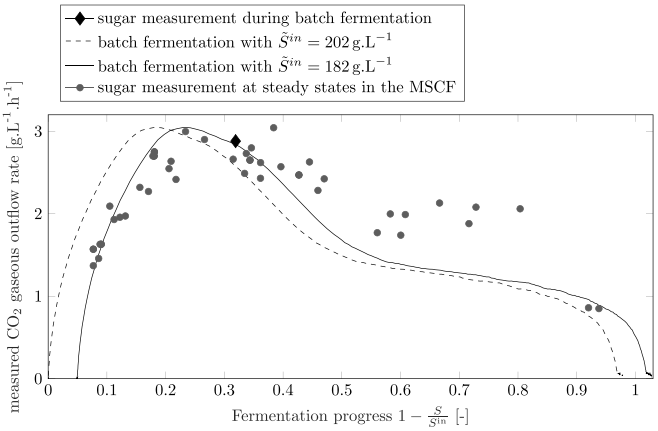

Fig. 5. Plot of the measured CO_2 gaseous outflow rate versus the fermentation progress $1 - (S/S^{\mathrm{in}})$ with $S = \tilde{S}^{\mathrm{in}} - k_2 \mathrm{CO}_2$ for $S^{\mathrm{in}} = 202$ $\mathrm{g.L}^{-1}$ and for the different values of $\tilde{S}^{\mathrm{in}}$ during some batch fermentations. Comparison with some sugar measurement data.

202 and 182 $\mathrm{g.L}^{-1}$. As we can see, the estimated values of S obtained with $\tilde{S}^{\mathrm{in}} = 182$ $\mathrm{g.L}^{-1}$ give much better results than the other ones. The value of $\tilde{S}^{\mathrm{in}}$ can obviously be adjusted more precisely either by an off-line estimation or even by an online estimation (with a Kalman filter for example). In the experiments presented in Section VI-D, the value of 182 $\mathrm{g.L}^{-1}$ was used, which greatly improved the results compared to the one presented in [13].

In the sequel, we will no more distinguish the CO_2 gaseous outflow rate from the CO_2 production rate for simplicity.

C. Numerical Tests

For the numerical experiments, we used different parameter sets for the control law and for the simulation of the MSCF, for which we apply the control law, in order to test the robustness to parameter uncertainty of the control strategy. The parameter set used for the control law is the one given in (9). The one used for the simulation of the MSCF is given by

$$\begin{aligned} k_1 &= 0.0606, \quad k_2 = 2.17, \ \mu_1^{\max} = 1.34\ [\mathrm{h}^{-1}] \\ \mu_2^{\max} &= 1.45\ [\mathrm{h}^{-1}], \ k_n = 1.57\ [\mathrm{g.L}^{-1}] \\ k_s &= 0.0154\ [\mathrm{g.L}^{-1}], \ k_e = 14.1\ [\mathrm{g.L}^{-1}]. \end{aligned} \quad (41)$$

As shown in [13, Fig. 3], the trajectories simulated with this parameter set fit well the experimental data of the batch fermentation.

For the control law and the Kalman filter, we used the following parameter values, $\forall i = 1:4$:

$$a_{i,1} = 1.2\ [\mathrm{h}^{-1}], \quad a_{i,2} = 0.25\ [\mathrm{h}^{-2}], \ \sigma = 0.2 \text{ and } \varepsilon = 0.64. \quad (42)$$

For the set of parameters (41), the constant inlet flow values Q_i^{OL}, $i = 1:4$, which leads at equilibrium to the set-point (35), have been computed and are given by

$$\left(Q_1^{OL}, Q_2^{OL}, Q_3^{OL}, Q_4^{OL}\right) = (0.2016, 0.1541, 0.0983, 0.0755). \quad (43)$$

TABLE III

STABILIZATION TIME AT 2% AND 5% FOR THE DIFFERENT SATURATION ORDERS IN CLOSED LOOP AND FOR THE OPEN-LOOP CONTROL LAW

	Saturation order in closed loop				Open
	$\{10,11,12,13,14\}$	$\{4,5\}$	$\{2,7\}$	$\{1,3,6,8,9\}$	loop
2%	8.0	8.2	8.6	15.9	43.8
5%	6.6	6.7	6.9	14.0	30.6

These inlet flow values fulfill the constraint (36), which makes the set-point (35) reachable.

The impact of the saturation order on the stabilization time has been evaluated through numerical simulations in the noise-free case (see Table III). The quickest stabilization time is obtained for the saturation orders $n°10$ to 14. The antiwindup input–output linearization control law gives better results than the open-loop control law in terms of the stabilization time. However, the difference between closed loop and open loop varies depending on the chosen set-point, the closed-loop control law being always at least as fast as the open-loop control law.[5]

For the experiments, the order $n°14$ has therefore been chosen. Some simulations obtained with this saturation order are shown in Fig. 6. For these simulations, we considered noisy measurements of the CO_2 production rates, the measurement noise having a zero-mean normal distribution with standard deviation $\sigma = 0.1$.

In Fig. 6 (top), the sugar concentration obtained with the antiwindup input–output linearization control law is compared to the one obtained with the constant input flow rates Q^{OL}. We see that the MSCF is stabilizing at the set-point with both the closed loop and open-loop control laws, but the stabilization time is smaller with the closed-loop strategy, as it was already shown in Table III. In Fig. 6 (middle), the values of the control input are plotted; we can verify that the constraint (1) is fulfilled all along the simulation. Finally, the noisy measurement values of the CO_2 production rate are shown in Fig. 6 (bottom).

In these simulations, the parameter sets used for the simulation of the MSCF and for the control law are different, and the measurements of the CO_2 production rate are noisy. It shows that the antiwindup input–output linearization control law is robust to both parameter uncertainties and measurement noise.

D. Experimental Results

The same experiment as the one tested in simulation has been performed on the real process. The sugar concentration in each reactor has been measured before applying the control law; the measurement values (given in Table IV, time 0) have been used for the initialization of the Kalman filter. During the experiment, two other off-line measurements of the sugar concentration have been made at 23.0 h and 38.7 h, respectively (see Table IV).

[5]The minimal time synthesis for the control of the yeast biomass (and not the one of the sugar) in an MSCF with only two reactors has been studied in [17]. It presents bang-bang and singular arcs, which makes it sensitive to error measurements and therefore difficult to implement in practice.

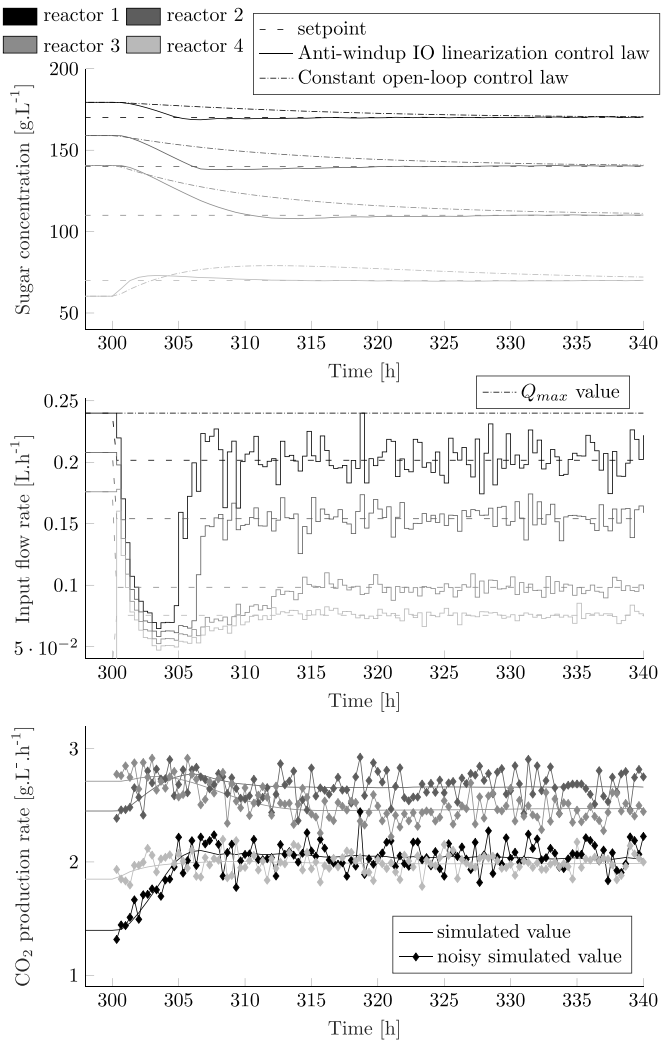

Fig. 6. Numerical results of the control of the sugar concentrations in the four reactors of the MSCF. Top: sugar concentration—comparison between open-loop control and antiwindup input–output control. Middle: control input values. Bottom: CO_2 production rate values (real and noisy).

TABLE IV

SUGAR CONCENTRATIONS MEASUREMENT DATA

Measurement time [h]	Sugar concentrations [g.L^{-1}]			
	S_1	S_2	S_3	S_4
0	185.8	161.5	140.4	58.6
23.0	174.56	140.69	108.19	69.1
38.7	174.77	140.10	106.32	66.9

The experimental results are presented in Fig. 7. The estimated sugar concentrations given by the observer are first plotted in Fig. 7 (top). In Fig. 7 (middle and bottom), the computed control input values Q_i and the online measurement of the CO_2 production rates C_i are given.

The measurements of the final sugar concentrations are given in Table V for comparison with the set-point values. As we can see, the qualitative behavior of the control law is good and similar to the one obtained in numerical simulation. However, without any online sugar concentration measurement, it is not possible to completely cancel the control

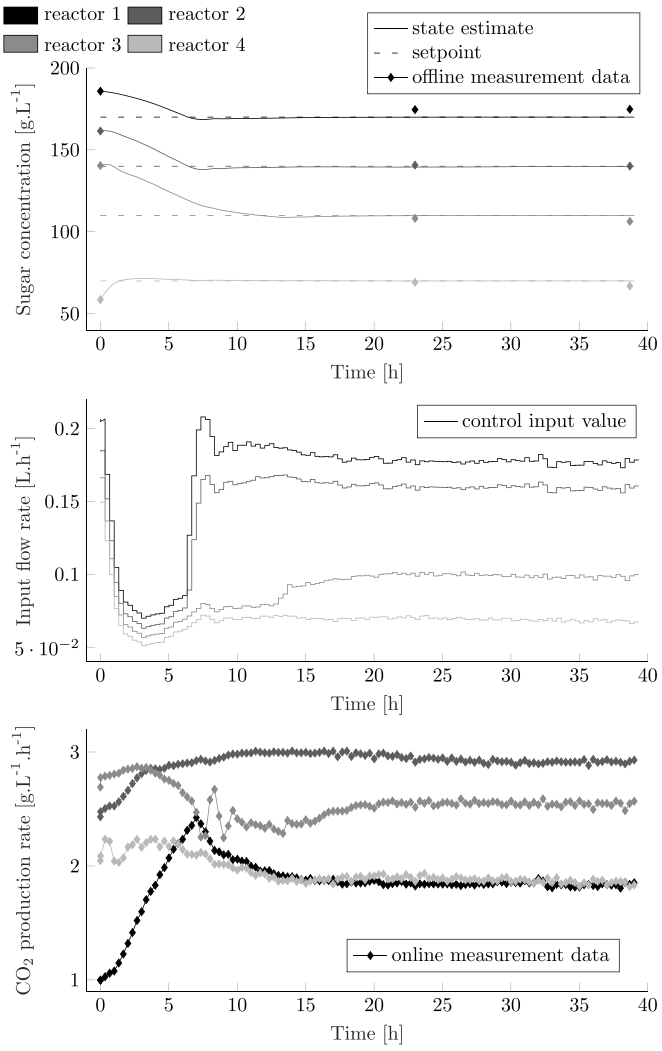

Fig. 7. Experimental results of the control of the sugar concentrations in the four reactors of the MSCF. Top: sugar concentration (set-point, estimated value, and offline measurements). Middle: control input values. Bottom: measurement values of the CO_2 production rate.

TABLE V
SUGAR CONCENTRATION SET POINTS AND FINAL MEASUREMENTS, VOLUMES, AND INITIAL DILUTION RATES OF THE EXPERIMENT

Reactor number	Sugar concentration [g.L^{-1}] with $S_0 = S_0^* = 202$ g.L^{-1}					
				$\delta_i^* :=$	$\delta_i :=$	
i	S_i^*	S_i	$S_i - S_i^*$	$S_i^* - S_{i-1}^*$	$S_i - S_{i-1}$	$\delta_i - \delta_i^*$
1	170	174.77	4.77	32	27.23	−4.77
2	140	140.10	0.1	30	34.67	4.67
3	110	106.32	−3.68	30	33.78	3.78
4	70	66.9	−3.1	40	39.42	−0.58

error, which is even though smaller than 4.77 g.L^{-1} in all the reactors. The uncertainty on sugar measurements being 3%, the control error, which is equal to 2.8%, 0.07%, 3.5%, and 4.4% in the four reactors, is reasonable.

E. Importance of the Value of S^{in} for the Control Error

Because of the cascade structure of the system, the control strategy proposed in this paper does not really control the sugar concentration in each reactor but rather the differences of sugar concentration between two consecutive reactors. The comparison between the values of the difference between consecutive set-points and measurements is given in Table V. We can see that the control errors are different if we look at the sugar concentration values or at the difference of sugar concentration values between the two consecutive reactors. For the second reactor, for example, the control error on the sugar concentration is only 0.1 g.L^{-1}, whereas the control error on the difference of sugar concentration with the first reactor is equal to 4.67 g.L^{-1}.

In fact, as the sugar concentration is not directly controlled, it implies that the control error on the sugar concentration in the ith reactor will depend on the control error of the preceding reactor (the $(i-1)$th reactor). To illustrate that, we can have a look at another experiment performed on the MSCF that we have presented in the conference paper [13]. In this experiment (see [13, Table II]), the control error on the sugar concentration was larger than 6 g.L^{-1} for all the reactors, whereas the control error on the difference of sugar concentration was smaller than 2.1 g.L^{-1} for all the reactors except for the first one for which the error was equal to 6.1 g.L^{-1}. In that case, the control error on the sugar concentration of the first reactor was clearly impacting the errors made on the other reactors.

As we suspected, the large control error obtained for the first reactor in this experiment was the consequence of both the variation of the yield coefficient k_2 during the fermentation (see Section IV) and the underestimation of the quantity of CO_2 that is dissolved in the medium (see Section VI-B). Indeed, for this experiment, we only decreased the value of S^{in} of 3 g.L^{-1}, whereas in the experiments presented in Section VI-D, 10 g.L^{-1} was subtracted.

VII. CONCLUSION

In this paper, the control of the sugar concentration in an MSCF has been studied. The cascade structure of the system induces a constraint on the control inputs that are the input flow rates of each reactor; the inlet flow rate of one reactor is indeed necessarily lower than that of the preceding reactor. To solve this problem, a linearizing control law coupled with an observer (Kalman filter) and an antiwindup mechanism was applied to the real process. The obtained results are convincing. However, because of the lack of online measurement of the sugar concentration, we have noticed the sensitivity of the results to the value of the initial sugar concentration. This value is not always well known, and moreover, it has to be corrected in order to take into account that a part of the produced CO_2 is dissolved in the medium. In order to make the control law more robust to this uncertainty, an adaptive control law could be proposed, which would adjust online the value of the initial sugar concentration. Another interesting perspective would be to test and compare other control strategies that have been recently proposed in [18] and [19]. Finally, the next objective for the control of the MSCF will be to control both the sugar concentration and the CO_2 production rate in each of the reactors.

REFERENCES

[1] G. Bastin and D. Dochain, *On-Line Estimation and Adaptive Control of Bioreactors*. Amsterdam, The Netherlands: Elsevier, 1990.

[2] G. Olsson and B. Newell, *Wastewater Treatment Systems: Modelling, Diagnosis and Control*. IWA Publishing, 1999.

[3] P. Vigie, G. Goma, P. Renaud, G. Chamilothoris, B. Dahhou, and J. Pourciel, "Adaptive predictive control of a multistage fermentation process," *Biotechnol. Bioeng.*, vol. 35, no. 3, pp. 217–223, 1990.

[4] I. Simeonov and S. Stoyanov, "Modelling and extremum seeking control of a cascade of two anaerobic bioreactors," *Int. J. Bioautomation*, vol. 15, no. 1, pp. 13–24, 2011.

[5] C. de Gooijer, W. Bakker, H. Beeftink, and J. Tramper, "Bioreactors in series: An overview of design procedures and practical applications," *Enzyme Microbial Tech.*, vol. 18, no. 3, pp. 202–219, 1996.

[6] S. Tarbouriech and M. Turner, "Anti-windup design: An overview of some recent advances and open problems," *IET Control Theory Appl.*, vol. 3, no. 1, pp. 1–19, 2009.

[7] F. Blanchini, "Set invariance in control," *Automatica*, vol. 35, no. 11, pp. 1747–1767, Nov. 1999.

[8] Y.-Y. Cao and Z. Lin, "Robust stability analysis and fuzzy-scheduling control for nonlinear systems subject to actuator saturation," *IEEE Trans. Fuzzy Syst.*, vol. 11, no. 1, pp. 57–67, Feb. 2003.

[9] S. Bezzaoucha, B. Marx, D. Maquin, and J. Ragot, "Stabilization of nonlinear systems subject to actuator saturation," in *Proc. FUZZ-IEEE*, Hyderabad, India, Jul. 2013, pp. 1–6.

[10] F. J. Doyle, "An anti-windup input–output linearization scheme for SISO systems," *J. Process Control*, vol. 9, no. 3, pp. 213–220, 1999.

[11] M. A. Henson and D. E. Seborg, *Nonlinear Process Control*. Upper Saddle River, NJ, USA: Prentice-Hall, 1997, pp. 149–231.

[12] A. Zheng, M. V. Kothare, and M. Morari, "Anti-windup design for internal model control," *Int. J. Control*, vol. 60, no. 5, pp. 1015–1024, 1994.

[13] C. Casenave, D. Dochain, J. Harmand, M. Perez, A. Rapaport, and J.-M. Sablayrolles, "Control of a multi-stage continuous fermentor for the study of the wine fermentation," in *Proc. IFAC WC*, Cape Town, South Africa, 2014, pp. 6192–6197.

[14] T. Clement, M. Perez, J.-R. Mouret, J.-M. Sablayrolles, and C. Camarasa, "Use of a continuous multistage bioreactor to mimic winemaking fermentation," *Int. J. Food Microbiol.*, vol. 150, no. 1, pp. 42–49, 2011.

[15] R. David, D. Dochain, J.-R. Mouret, A. Vande Wouwer, and J.-M. Sablayrolles, "Dynamical modeling of alcoholic fermentation and its link with nitrogen consumption," in *Proc. CAB*, Leuven, Belgium, 2010, pp. 496–501.

[16] J.-P. Corriou, *Process Control: Theory and Applications*. London, U.K.: Springer-Verlag, 2004.

[17] T. Bayen, A. Rapaport, and M. Sebbah, "Minimal time control of the two tanks gradostat model under a cascade input constraint," *SIAM J. Control Optim.*, vol. 52, no. 4, pp. 2568–2594, 2014.

[18] C. Casenave and M. Perez, "Control of a class of nonlinear cascade systems with input-dependent saturations," in *Proc. CCDC*, Qingdao, China, 2015, pp. 131–136.

[19] C. Casenave and E. Montseny, "Simplification of dynamic problems by time-scale transformation: Application to the nonlinear control with input positive constraints," in *Proc. IFAC WC*, Toulouse, France, 2017, pp. 10691–10696.

Authors' photographs and biographies not available at the time of publication.